

PAPER

Gate-first process compatible, high-quality *in situ* SiN_x for surface passivation and gate dielectrics in AlGaN/GaN MISHEMTs

To cite this article: Liang Cheng *et al* 2019 *J. Phys. D: Appl. Phys.* **52** 305105

View the [article online](#) for updates and enhancements.

You may also like

- [GaN-based power high-electron-mobility transistors on Si substrates: from materials to devices](#)
Nengtao Wu, Zhiheng Xing, Shanjie Li et al.
- [Review—Silicon Nitride and Silicon Nitride-Rich Thin Film Technologies: State-of-the-Art Processing Technologies, Properties, and Applications](#)
Alain E. Kaloyeros, Youlin Pan, Jonathan Goff et al.
- [Review—Silicon Nitride and Silicon Nitride-Rich Thin Film Technologies: Trends in Deposition Techniques and Related Applications](#)
Alain E. Kaloyeros, Fernando A. Jové, Jonathan Goff et al.



ECS
The
Electrochemical
Society
Advancing solid state &
electrochemical science & technology

DISCOVER
how sustainability
intersects with
electrochemistry & solid
state science research

Gate-first process compatible, high-quality *in situ* SiN_x for surface passivation and gate dielectrics in AlGaN/GaN MISHEMTs

Liang Cheng¹, Weizong Xu¹, Danfeng Pan¹, Youhua Zhu², Fangfang Ren¹, Dong Zhou¹, Jiandong Ye¹, Dunjun Chen¹, Rong Zhang¹, Youdou Zheng¹ and Hai Lu¹

¹ School of Electronic Science and Engineering, Nanjing University, Nanjing 210023, People's Republic of China

² School of Information Science and Technology, Nantong University, Nantong 226019, People's Republic of China

E-mail: wz.xu@nju.edu.cn and hailu@nju.edu.cn

Received 28 January 2019, revised 17 April 2019

Accepted for publication 29 April 2019

Published 24 May 2019



CrossMark

Abstract

In the research of passivation/gate dielectrics for AlGaN/GaN based high electron mobility transistors (HEMTs), *in situ* SiN_x has specific advantages over *ex situ* SiN_x in terms of lower defects level and higher dielectric quality. In this paper, an *in situ* grown SiN_x layer as thick as 47 nm was deposited on AlGaN/GaN heterostructure by metalorganic chemical vapor deposition, with capabilities of functioning simultaneously as passivation and gate dielectrics verified. Systematical investigations have been performed on the *in situ* SiN_x in aspects of bulk dielectric quality, interface property and dielectric reliability. Correspondingly, high leakage suppression ability with leakage current $<10^{-8}$ A cm⁻² at 125 °C, near-ideal dielectric breakdown strength of ~ 13.2 MV cm⁻¹, high interface quality with state density of $\sim 3.0 \times 10^{12}$ eV⁻¹ cm⁻² have been revealed. In the dielectric reliability analysis, a maximum forward bias as high as 19.5 V (~ 3.66 MV cm⁻¹) for a ten-year lifetime at the failure level of 0.01% was obtained. Subsequent experiments also revealed the gate-first process compatibility of this high-quality *in situ* SiN_x, providing additional process convenience and design flexibility for AlGaN/GaN HEMTs.

Keywords: *in situ* SiN_x, AlGaN/GaN MISHEMT, passivation, gate dielectric, gate-first process

(Some figures may appear in colour only in the online journal)

1. Introduction

AlGaN/GaN based high electron mobility transistor (HEMT) is an attractive candidate for new-generation power switching and RF applications, given their superior material properties including high electron saturation velocity, high breakdown electric field and large sheet carrier densities [1]. However, the ultrathin AlGaN barrier generally suffers from surface sensitivity and leads to large gate leakage currents as well as current collapse, requiring effective passivation technology [2–4]. It is also beneficial to adopt a gate dielectric layer to suppress the gate leakage and to increase on-state gate swing range, composing metal-insulator-semiconductor

HEMT (MIS-HEMT). SiO₂ and SiN_x deposited with plasma enhanced chemical vapor deposition (PECVD) are the most commonly used passivation/gate dielectric materials in GaN HEMTs [2, 5]. However, the *ex situ* fabrication approach may introduce additional growth- and process-related contaminations or defects on the devices, enhancing shallow-traps related leakage paths at the AlGaN surface [6]. Comparatively, *in situ* grown SiN_x in the metalorganic chemical vapor deposition (MOCVD) system immediately after the AlGaN/GaN heterostructure growth promises numerous advantages. This *in situ* process could prevent the as-grown GaN HEMT barrier layer from being exposed to ambient air, thus effectively eliminating the process-related

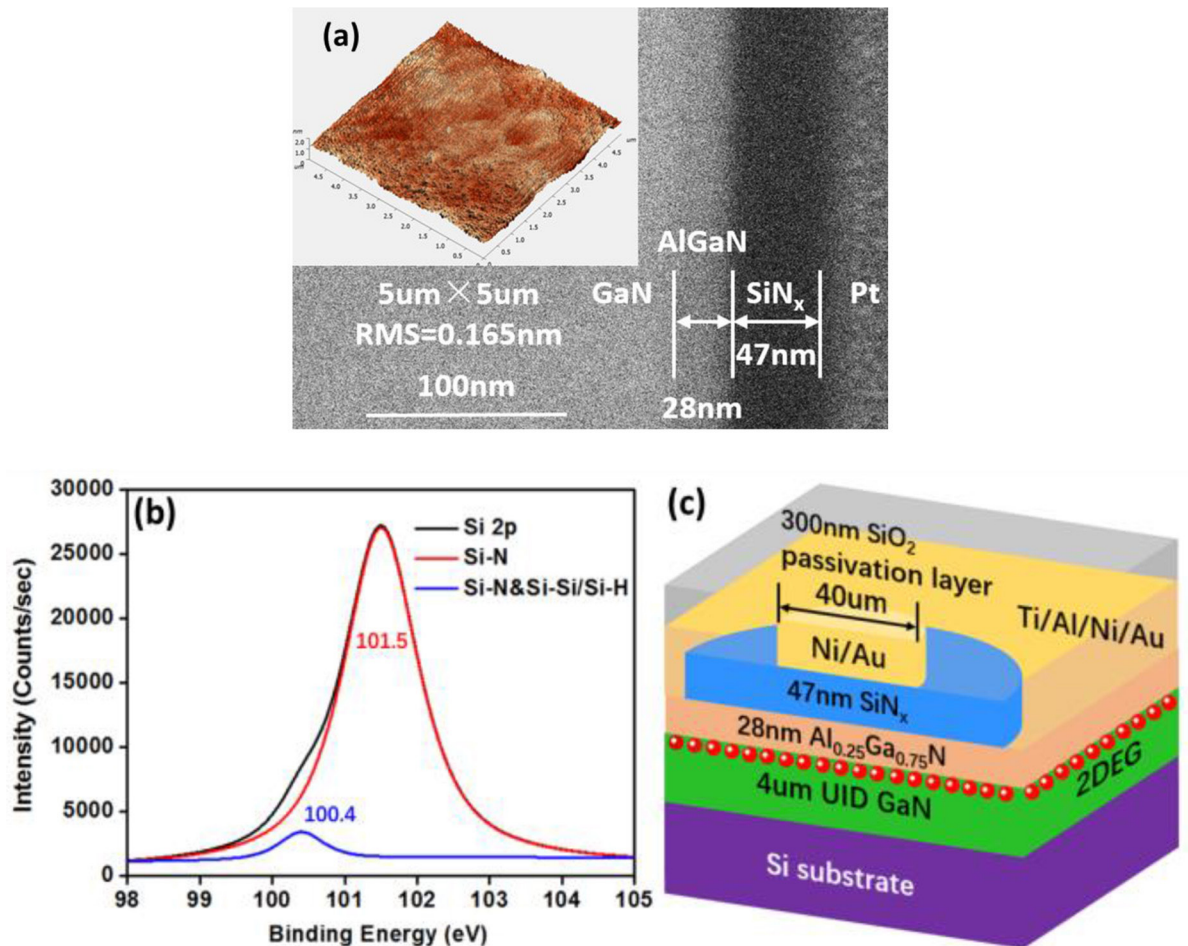


Figure 1. (a) SEM image of the epitaxial structure covered with Pt, the inset shows the AFM image of the SiN_x surface with a RMS roughness of 0.165 nm within a 5 μm × 5 μm area. (b) The fitting XPS result of Si 2p core-level spectrum of the MOCVD *in situ* SiN_x film. (c) Schematic cross-sectional view of the SiN_x/AlGaN/GaN MIS diode.

contamination and damage. Meanwhile, the higher growth temperature and lower deposition rate could obtain better SiN_x dielectric quality [7, 8]. Nevertheless, limited thickness of the strained SiN_x on AlGaN is a critical issue for realizing its fundamental benefits as expected [7]. Combinations of *in situ* SiN_x and *ex situ* SiN_x by PECVD [7] or LPCVD [9] have been proposed to equivalently increase the SiN_x thickness, however, would still introduce additional process complexity. Therefore, properties and functionalities of thick *in situ* SiN_x deserve comprehensive investigations.

In this work, an *in situ* MOCVD SiN_x layer as thick as 47 nm was deposited on AlGaN/GaN heterostructure, and systematical investigations have been performed in terms of bulk dielectric quality, interface property and reliability. Dielectric leakage current density of ~10⁻⁸ A cm⁻² and breakdown electric field (E_B) of ~13.2 MV cm⁻¹ was revealed in current–voltage (I – V) measurements, illustrating the strong leakage-suppression ability and high breakdown strength. Subsequent frequency/temperature-dependent capacitance–voltage (C – V) measurements have obtained a low interface state density (D_{it}) of ~3.0 × 10¹² eV⁻¹ cm⁻². Excellent dielectric reliability has also been verified in the following time-dependent dielectric breakdown (TDDB) tests. All of these benefits demonstrate its advantageous applications as

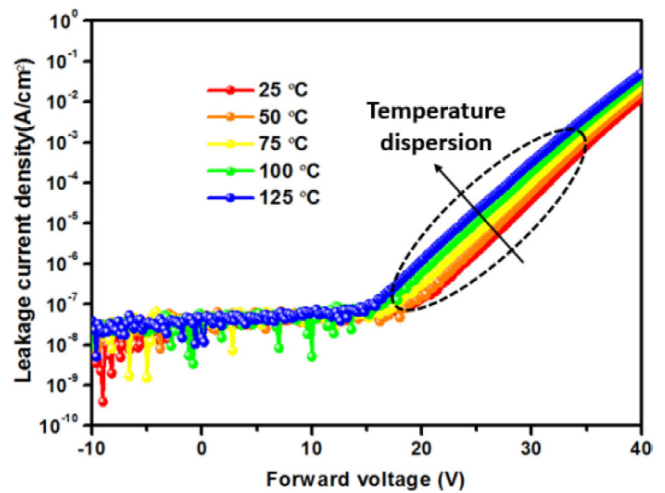


Figure 2. Temperature-dependent JV characteristics of the MOCVD *in situ* SiN_x/AlGaN/GaN MIS diode.

passivation layer and gate dielectrics in AlGaN/GaN heterostructure based devices.

Ultimately, gate-first process compatibility has been explored and verified. It was found that the *in situ* SiN_x could tolerate the high-temperature ohmic metal annealing process with

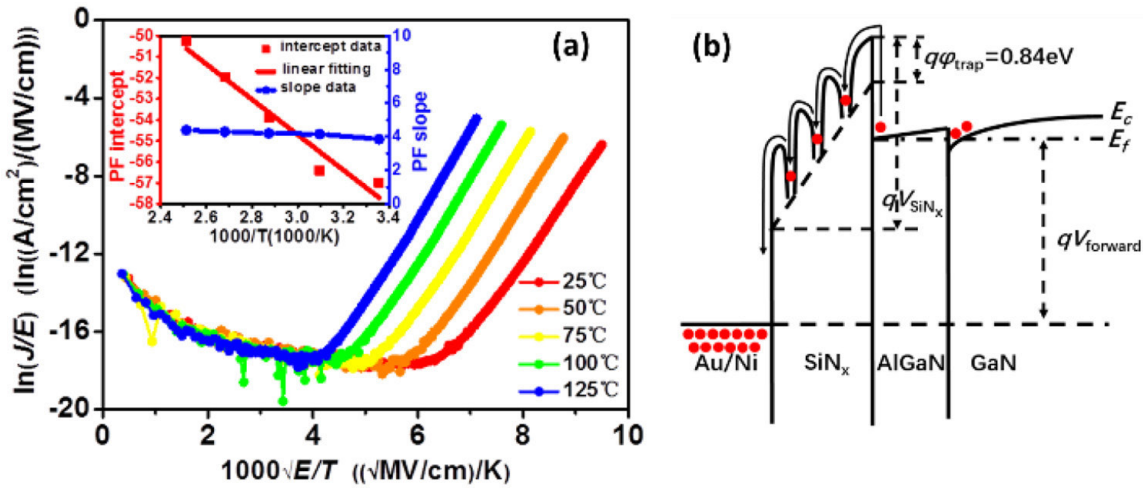


Figure 3. (a) PF plots $\ln(J/E)$ versus $1000\sqrt{E/T}$ of the MOCVD *in situ* $\text{SiN}_x/\text{AlGaIn}/\text{GaIn}$ MIS diode. Inset: PF slope and intercept extracted from linear fitting. (b) Energy band diagram of the PF emission dominated leakage at low electric field.

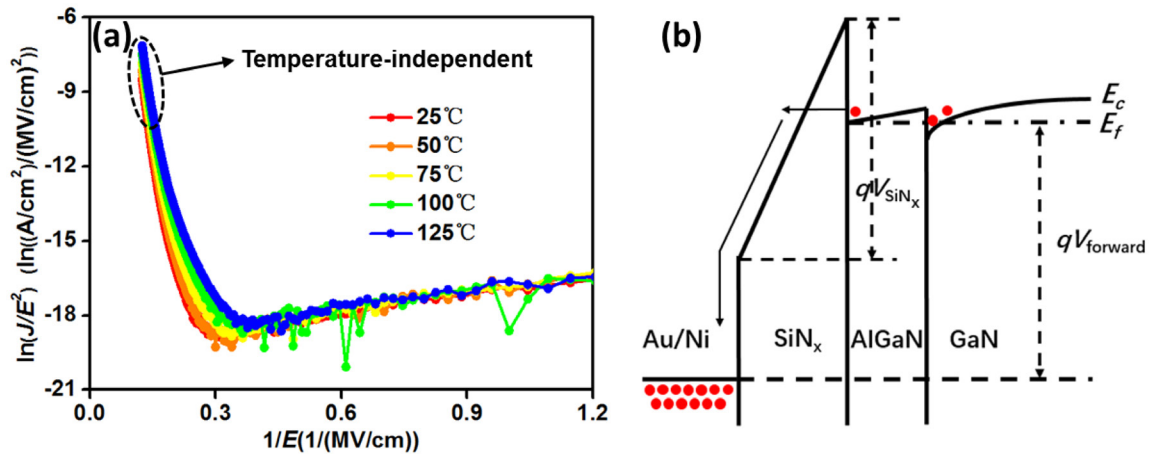


Figure 4. (a) FN plots $\ln(J/E^2)$ versus $1/E$ of *in situ* $\text{SiN}_x/\text{AlGaIn}/\text{GaIn}$ MIS diode at temperature from 25 °C to 125 °C with the step of 25 °C. (b) Energy band diagram of the FN tunneling dominated leakage at high electric field.

Ni/Au on its surface, while little degradation could be observed in dielectric properties. Therefore, it is believed that this *in situ* SiN_x presents a new roadmap for technology optimization in both AlGaIn/GaN HEMT passivation and gate dielectrics, facilitating the advances in device performance and applications.

2. Device structure and fabrication

The cross-section scanning electron microscopy (SEM) image of the deposited $\text{SiN}_x/\text{AlGaIn}/\text{GaIn}$ layers is shown in figure 1(a). The epitaxial structure was grown on a 6-inch Si substrate with thickness of 1 mm in high temperature MOCVD. It consists of a 4 μm GaN buffer layer, a 300nm GaN channel layer, a 28nm $\text{Al}_{0.25}\text{Ga}_{0.75}\text{N}$ barrier layer, and a 47 nm *in situ* SiN_x cap dielectric, which is deposited with a proprietary recipe. The *in situ* SiN_x was deposited subsequent to the growth of AlGaIn/GaN heterostructure in the MOCVD chamber with a substrate temperature of 1150 °C, a chamber pressure of 120 mTorr and a SiH_4/NH_3 ratio of $\sim 4 \times 10^{-6}$. The growth rate of the SiN_x is

$\sim 2 \text{ \AA min}^{-1}$. The film index of the *in situ* SiN_x is determined to be 1.95 via variable angle spectroscopic ellipsometry measurements. The 2DEG concentration of the AlGaIn/GaN heterostructure is measured to be $\sim 5.7 \times 10^{12} \text{ cm}^{-2}$. The inset in Figure 1(a) shows an AFM image of the as-grown SiN_x film, with a root mean square (RMS) roughness of 0.165 nm within a $5 \mu\text{m} \times 5 \mu\text{m}$ area. X-ray photoelectron spectroscopy (XPS) measurements were performed on the SiN_x surface of the epitaxial layers in order to determine the N/Si ratio. With C 1s peak energy calibrated to 285 eV, a typical Si 2p core-level XPS spectrum has been captured, as shown in figure 1(b). Two components with the peak energy positions of 101.5 eV and 100.4 eV could be extracted from the spectrum, corresponding to Si–N bonds and a mixing of Si–N and Si–Si or Si–H bonds respectively [6, 10]. The comprehensive analysis indicates that the *in situ* SiN_x film has a N/Si ratio of 1.24, similar to the values as reported in the previous literature, where SiN_x has high quality but small thickness [6, 11]. Corresponding metal-insulator-semiconductor (MIS) diodes based on Au/Ni/ $\text{SiN}_x/\text{AlGaIn}/\text{GaIn}$ stacks were fabricated with the ohmic electrode electrically connected to 2DEG (see figure 1(c)). During the fabrication,

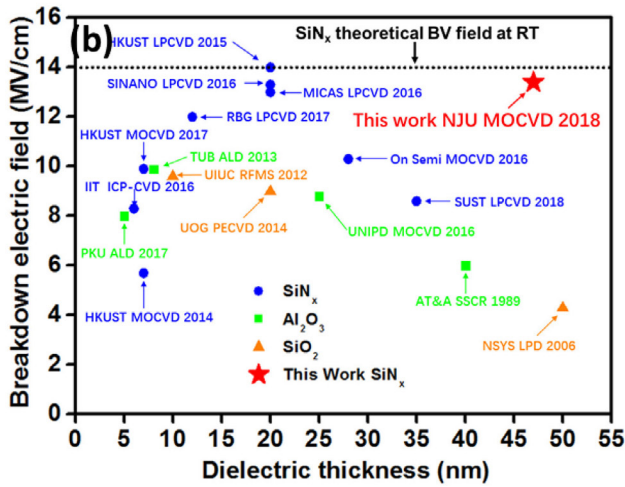
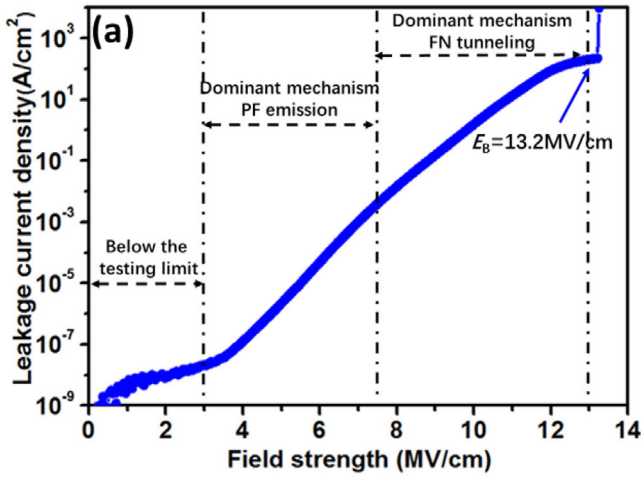


Figure 5. (a) Leakage current density versus electric field strength of *in situ* SiN_x at room temperature (RT). (b) Benchmark of dielectric breakdown strength for SiN_x, Al₂O₃, SiO₂ fabricated with different techniques in recent reports [6, 7, 14–27].

CF₄-based reactive ion etching (RIE) was firstly performed on the wafer to selectively remove the SiN_x dielectric layer in the ohmic contact region. The wafer was then treated with 10% TMAH solution at 80 °C for 30 min to repair the etching damage. Subsequently, Ti/Al/Ni/Au (40/80/40/100 nm) ohmic electrode was deposited with e-beam evaporation and annealed at 850 °C in N₂ ambient for 30 s. Finally, the top electrode of Ni/Au (40/100 nm) with the diameter of 40 μm was defined and deposited upon the *in situ* SiN_x layer.

3. Device results and discussion

3.1. Bulk dielectric quality of *in situ* SiN_x

Functionality and effectiveness of the *in situ* SiN_x dielectric as a passivation layer rely on the bulk properties of the dielectric and the dielectric/III-nitride interface quality. Therefore, dielectric leakage level was firstly evaluated. Figure 2 gives the leakage current density (*J*) versus voltage bias (*V_F*) on the MIS-diode, at various temperatures from 25 °C to 125 °C with the step of 25 °C. It could be observed that,

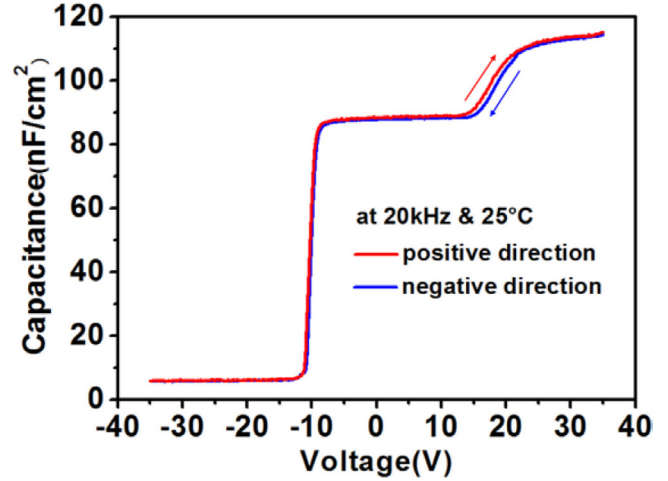


Figure 6. Bidirectional CV hysteresis characteristics of the MOCVD *in situ* SiN_x/AlGaIn/GaN MIS diode at 20 kHz and 25 °C.

even at 125 °C and *V_F* = 15 V, the dielectric leakage is suppressed below the testing limit of the measuring system, i.e. *J* < 10⁻⁸ A cm⁻², indicating the extremely high leakage resistivity of the *in situ* grown SiN_x. At *V_F* > 15 V, the leakage current reaches the testing limit and rises with the increasing *V_F*, which should be attributed to the strong accumulation in the 2DEG channel and electron spilling over the AlGaIn barrier. It could be noted in figure 2 that the *J*-*V* curves exhibit observable temperature dispersion at *V_F* ~ 20 V, indicating the dominant leakage mechanism in this voltage region should be temperature related. To further identify the dielectric leakage mechanism, detailed analysis was carried out.

Figure 3(a) gives the Poole–Frenkle (PF) emission model fitting of the dielectric leakage. Here, the PF emission leakage current can be expressed by [12]:

$$J_{PF} \propto E_{SiN_x} \exp \left[-\frac{q \left(\phi_{trap} - \sqrt{q E_{SiN_x} / \pi \epsilon_{SiN_x}} \right)}{kT} \right] \quad (1)$$

where *E_{SiN_x}*

 is the electric field strength in SiN_x, ε_{SiN_x} is the dielectric constant of SiN_x, *k* is the Boltzmann constant, *T* is the absolute temperature, and *qφ_{trap}* is the effective barrier height for the electron emission, as illustrated in figure 3(b). The transformation from *V_F* to *E_{SiN_x}* was based on numerical simulations with the commercially available TCAD Silvaco. As could be observed, the dielectric leakage fits PF plots well with near uniform slope of 4 for different *T*, as illustrated with blue curve in the inset of figure 3(a). Resultantly, based on the intercept values deduced in the PF fitting in the inset of figure 3(a) (red curve), the *qφ_{trap}* for the electron emission from the trap states is extracted to be 0.84 eV.

As the *V_F* further increases, *J*-*V* curves merge again (see figure 2), where the Fowler–Nordheim model with ln(*J*/*E*²) versus 1/*E* plots show excellent linear fitting, being independent of *T* at higher electric field strength. Therefore, at higher *V_F* and larger electric field, direct tunneling process dominates the leakage, which is consistent with previous reports [13, 14].

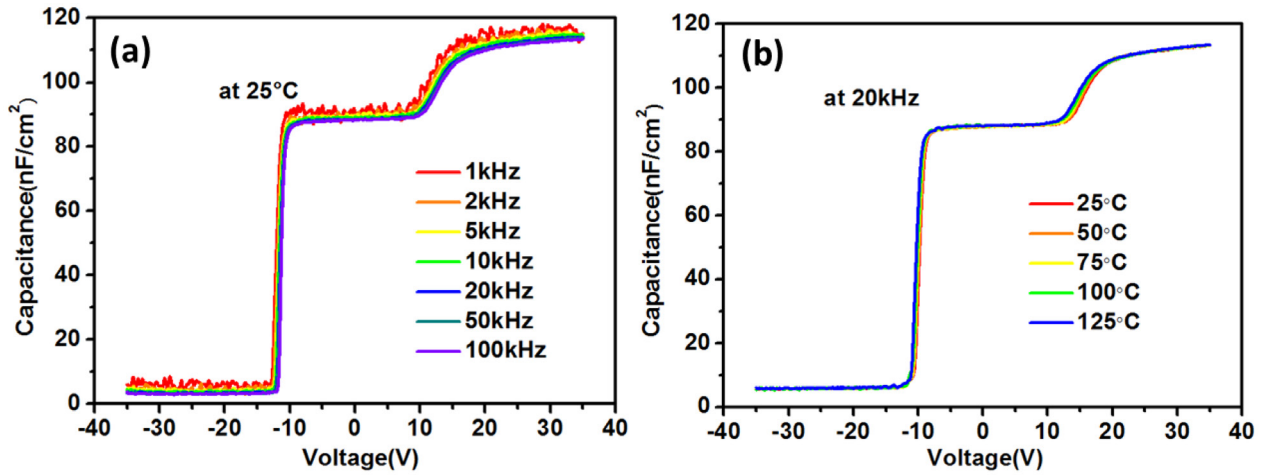


Figure 7. CV characteristic of the MOCVD *in situ* Si_x/AlGaIn/GaN MIS diode. (a) Frequency-dependent CV curves at 25 °C. (b) Temperature-dependent CV curves at 20 kHz.

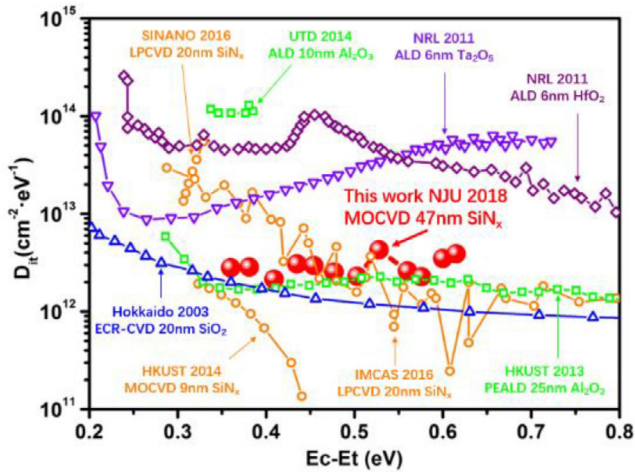


Figure 8. Benchmark of D_{it} mapping of different dielectric/III-nitride interfaces [15, 31–36].

Abrupt permanent dielectric breakdown occurred with V_F reaching 64.4 V, revealing a breakdown electric field (E_B) of ~ 13.2 MV cm⁻¹ (see figure 5(a)). This value is very close to the theoretically predicted E_B value of ~ 14 MV cm⁻¹ for Si_xN_y [28], demonstrating the high bulk quality of the *in situ* grown Si_xN_y dielectric. Figure 5(b) shows a benchmark for the state-of-art E_B values of Si_xN_y as well as SiO₂, Al₂O₃, those adopted as passivation or gate dielectrics on GaN HEMTs. It could be concluded that, in spite of the thickness as high as 47 nm, E_B of the fabricated *in situ* Si_xN_y layer is among the best values as compared with those *ex situ* or thin *in situ* Si_xN_y, being very promising for high-voltage GaN devices passivation applications.

3.2. Dielectric/III-nitride interface quality

Si_xN_y/AlGaIn interface quality was then investigated, mainly through interface state density (D_{it}) mapping in frequency/temperature-dependent CV measurements. First of all, bidirectional CV hysteresis measurements were carried out on the *in situ*

Si_xN_y/AlGaIn/GaN MIS diodes, as shown in figure 6. The typical CV characteristics for the MIS diode based on AlGaIn/GaN heterostructure feature two unique rises near $V_F = -11$ V and 12 V, respectively. With V_F increasing forwardly to above -11 V, the 2DEG channel changes from pinch-off state to accumulation, where the measured capacitance (C_{MIS}) can be regarded as a combination of AlGaIn barrier capacitance (C_{AlGaIn}) and Si_xN_y dielectric capacitance (C_{SiNx}), i.e. $1/C_{MIS} = 1/C_{AlGaIn} + 1/C_{SiNx}$. As V_F reaches above 12 V, the CV curve shows a second rise. This should be a result of the channel electrons spilling over AlGaIn barrier layer to the Si_xN_y/AlGaIn interface [29]. The Si_xN_y/AlGaIn interface states would then contribute to the C_{MIS} via interacting with the channel electrons. A small hysteresis could be observed in the bidirectional measurements, which should be a result of electron trapping process under the positive gate bias. Thus, interface-located trap states were revealed. To gain insight into the interfacial states properties, systematical frequency- and temperature-dependent CV measurements were performed on the *in situ* Si_xN_y/AlGaIn/GaN MIS diodes, with frequency varying from 1 kHz to 100 kHz and temperature varying from 25 °C to 125 °C.

As has been addressed in previous literature [30], the onset voltage of the second rise in CV curves would increase with higher measuring frequency and/or lower temperature. This is in good accordance with the experimental results, as shown in figures 7(a) and (b), where device threshold voltage exhibits remarkable stability at various temperatures. Based on the calculation model and formula in [12], which has also been widely applied and verified in Si MOSFETs, D_{it} is calculated to be $\sim 3.0 \times 10^{12}$ eV⁻¹ cm⁻² in energy level ($E_c - E_t$) ranging from 0.35 eV to 0.62 eV (see figure 8). As compared to other previously investigated dielectrics, including Si_xN_y, SiO₂, Al₂O₃, etc, the D_{it} obtained in this work is among the lowest values [15, 31–36]. Therefore, the *in situ* Si_xN_y/AlGaIn interface produced in this work has a relatively higher quality, which should be crucial for the stability and dynamic performance of the passivated AlGaIn/GaN MISHEMTs.

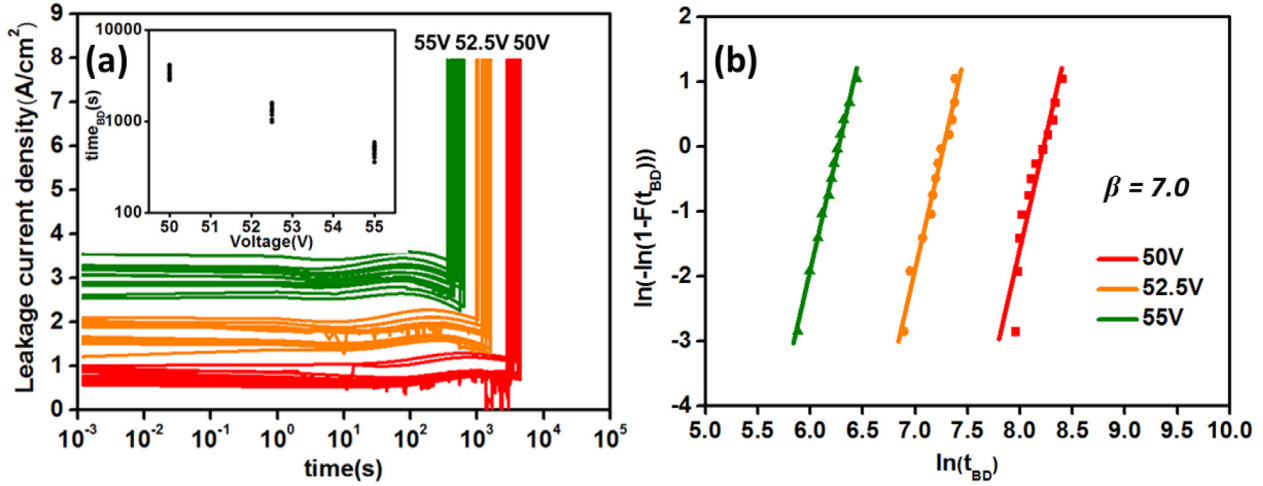


Figure 9. (a) Time-dependent dielectric leakage evolution of the 36 *in situ* SiN_x/AlGaIn/GaN MIS diodes at RT. The inset shows the statistic results of t_{BD} for different forward bias voltages. (b) Weibull distribution fitting for the t_{BD} results.

3.3. Reliability and lifetime prediction

The long-term reliability is another critical issue of passivation dielectrics. In this work, TDDB measurements were carried out on the MOCVD *in situ* AlGaIn/GaN MIS diodes at room temperature (25 °C), and the dielectric lifetime was predicted employing Weibull distribution statistics theory. As has been mentioned in section 3.1, the breakdown voltage of *in situ* SiN_x MIS diode is ~64.4 V. Then, 75%–85% of the breakdown voltages (50 V, 52.5 V, 55 V) was selected as the constant forward bias in TDDB measurements. The time to breakdown (t_{BD}) was defined at the abrupt increase in dielectric leakage. Time-dependent dielectric leakage evolution of 36 different MIS diodes (12 diodes for each bias condition) is given in figure 9(a). Statistics results suggest that the dielectric has average lifetime of about 4000 s, 1100 s, 550 s for bias voltage of 50 V, 52.5 V, 55 V, respectively.

Further investigation on the discrete t_{BD} values found that, the statistics fit well with Weibull distribution in the form of $\ln[-\ln(1-F(t_{BD}))] = \beta(\ln t_{BD} - \ln \eta)$, as shown in figure 9(b). The Weibull distribution is given by [15]:

$$F(t) = 1 - \exp\left[-\left(\frac{t}{\eta}\right)^\beta\right] \quad (2)$$

where $F(t)$ is the failure rate, β is the shape factor or the slope of Weibull distribution, η is scale factor that equals to the statistical time at 63% failure rate. From the fitting of Weibull plots, corresponding β (~7.0) and η could be obtained for each bias condition. Three η values have been obtained, and with \sqrt{E} model, the dielectric lifetime versus forward bias condition could be predicted [14]. Accordingly, the maximum forward bias for ten-year lifetime is extracted to be 19.5 V (~3.66 MV cm⁻¹) at a failure level of 0.01%, as shown in figure 10.

3.4. Gate dielectric applications and gate-first process capability

The above investigations on bulk dielectric quality, interface property and reliability of the *in situ* grown SiN_x have also

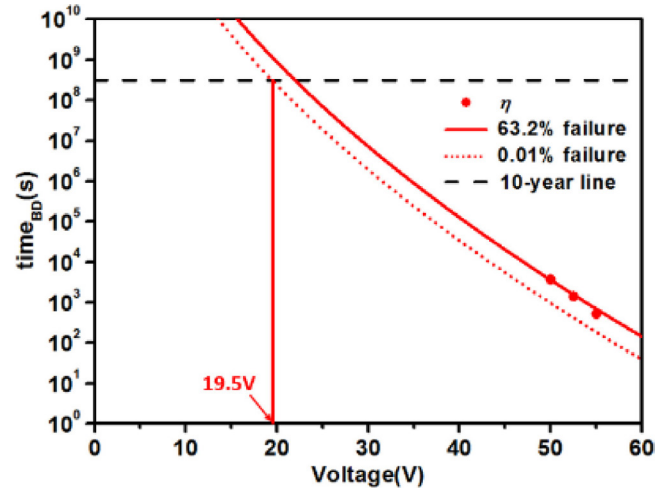


Figure 10. Lifetime prediction of the 0.01% failure level at room temperature employing \sqrt{E} model.

demonstrated its capability of being used as high-quality gate dielectric in GaN MISHEMTs, guaranteeing large gate swing range, low gate leakage, low D_{it} , and long dielectric lifetime. In further experiments, the gate-first process compatibility of the *in situ* SiN_x has been evaluated. As in the gate-first fabrication process, Ni/Au gate metal was firstly deposited on SiN_x, then the source/drain electrodes of Ti/Al/Ni/Au were deposited where SiN_x was removed with RIE for ohmic contacts. Finally, ohmic contact metallization was conducted at 850 °C in N₂ for 30 s. Therefore, in the gate-first process, the SiN_x has to go through the high-temperature annealing process with gate metal (Ni/Au) on its surface. As indicated in the electrical measurements performed on the subsequently fabricated gate-first GaN MIS diodes, the SiN_x gate dielectric exhibits little degradation. Breakdown electric field strength of ~12.6 MV cm⁻¹, D_{it} of $\sim 5.0 \times 10^{12}$ eV⁻¹ cm⁻², and the maximum forward bias for a ten-year lifetime of 16.7 V at the failure level of 0.01% has been observed. The slight variations could be a result of the Au migration through the Ni layer to the dielectric during the ohmic annealing [37], which, however should have been

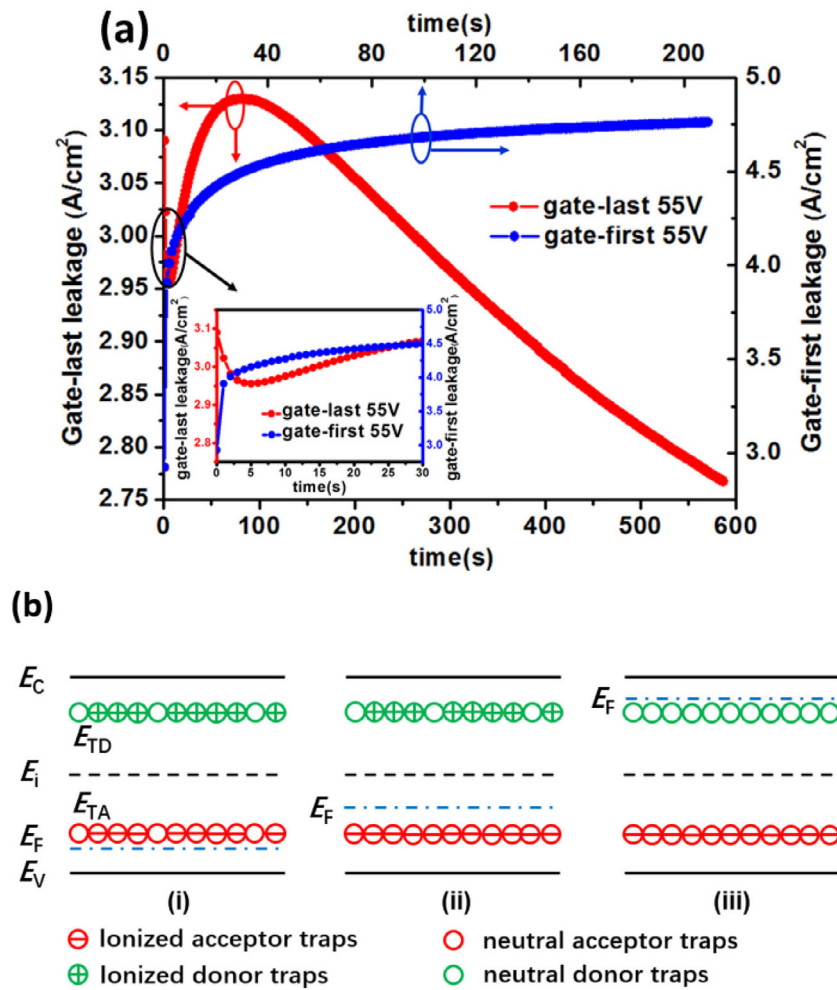


Figure 11. (a) $J-t$ characteristics of the *in situ* SiN_x/AlGaIn/GaN MIS diodes fabricated with gate-first (blue) and gate-last (red) process at room temperature. (b) Schematic diagram of the two trap levels, including acceptor and donor traps.

largely blocked by the high-quality *in situ* SiN_x. Thus, the *in situ* grown SiN_x is compatible with the gate-first process, promising higher process convenience and especially applicability of self-aligned technique [38].

Time-dependent leakage evolution of the *in situ* SiN_x has then been analyzed based on both gate-first and gate-last processed devices, at a constant forward bias of 55 V (near breakdown voltage of the dielectrics). As illustrated in figure 11(a), gate-first processed SiN_x exhibited continuously increasing leakage current (blue), which should be attributed to the accumulative dielectric damage with continuous electron injection. While for gate-last processed SiN_x, two falling stages have been observed (red). This should be a result of the state changes of the dielectric traps in the as-grown SiN_x (see figure 11(b)). That is, both acceptor-like and donor-like traps exist in the fabricated SiN_x layer (state i). At first, the injected electrons get captured in the neutral acceptor traps, resulting in ionization of acceptor traps (state ii). Then, the continuously injected electrons stimulate the neutralization of donor traps (state iii). Both these two stages would enhance the trap states electronegativity, restraining the leakage via Coulomb

scattering effect. This suggests that gate-first process should have modified the trap-related states in SiN_x, yet has little impact on the dielectric’s long-term reliability.

4. Conclusion

In this paper, a 47 nm-thick *in situ* SiN_x layer was grown on AlGaIn/GaN heterostructure by MOCVD with its dielectric properties systematically investigated. The excellent dielectric insulativity with ultra-low leakage level, near-ideal electric breakdown strength, low interface state density and long dielectric lifetime have been revealed, demonstrating its great potentials in passivation and gate dielectric applications for AlGaIn/GaN heterostructure based devices. Further study has also verified its compatibility with gate-first process, offering additional process convenience and design flexibility. Therefore, this proposed *in situ* grown SiN_x provides a fascinating substitute for optimizing the passivation and gate dielectrics, thus promising higher-performance AlGaIn/GaN based MISHEMTs.

Acknowledgments

This work was supported by the National Key R&D Program of China (No. 2017YFB0403000), the National Natural Science Foundation of China (Nos. 91850112 and 61774081), the Natural Science Foundation of Jiangsu Province, China (No. BK20161401), and the Fundamental Research Funds for the Central Universities (Nos. 021014380098, 021014380085 and 021014380093), the Priority Academic Program Development of Jiangsu Higher Education Institutions, and the Science and Technology Project of State Grid Corporation of China (SGSDDK00KJJS1600071).

ORCID iDs

Liang Cheng  <https://orcid.org/0000-0002-4059-585X>

Jiandong Ye  <https://orcid.org/0000-0002-3985-6768>

References

- [1] Wong K-Y R *et al* 2015 *Proc. IEEE Int. Electron Devices Meeting* pp 9.5.1–4
- [2] Lu X, Jiang H, Liu C, Zou X and Lau K M 2016 *Semicond. Sci. Technol.* **31** 055019
- [3] Huang T, Malmros A, Bergsten J, Gustafsson S, Axelsson O, Thorsell M and Rorsman N 2015 *IEEE Trans. Electron Devices* **36** 537–9
- [4] Kim H, Lee J, Liu D and Lu W 2005 *Appl. Phys. Lett.* **86** 143505
- [5] Arulkumaran S, Egawa T, Ishikawa H, Jimbo T and Sano Y 2004 *Appl. Phys. Lett.* **84** 613–5
- [6] Lu X, Ma J, Jiang H and Lau K M 2014 *Appl. Phys. Lett.* **104** 032903
- [7] Jiang H, Liu C, Chen Y, Lu X, Tang C W and Lau K M 2017 *IEEE Trans. Electron Devices* **64** 832–9
- [8] Lu X, Ma J, Jiang H, Liu C, Xu P and Lau K M 2015 *IEEE Trans. Electron Devices* **62** 1862–9
- [9] Wu T-L, Marcon D, Zahid M B, Hove M V, Decoutere S and Groeseneken G 2013 *IEEE Int. Reliability Physics Symp. (Anaheim, CA)* pp 3C.5.1–7
- [10] Beche E, Berjoan R, Viard J, Cros B and Durand J 1995 *Thin Solid Films* **258** 143–50
- [11] Lu X, Ma J, Jiang H, Liu C and Lau K M 2014 *Appl. Phys. Lett.* **105** 102911
- [12] Swain R, Jena K and Lenka T R 2016 *IEEE Trans. Electron Devices* **63** 2346–52
- [13] Hua M, Liu C, Yang S, Liu S, Fu K, Dong Z, Cai Y, Zhang B and Chen K J 2015 *IEEE Electron Device Lett.* **36** 448–50
- [14] Hua M, Liu C, Yang S, Liu S, Fu K, Dong Z, Cai Y, Zhang B and Chen K J 2015 *IEEE Trans. Electron Devices* **62** 3215–22
- [15] Zhang Z *et al* 2016 *IEEE Trans. Electron Devices* **63** 731–8
- [16] Liu Z *et al* 2016 *J. Vac. Sci. Technol. B* **34** 041202
- [17] Dutta G, DasGupta N and DasGupta A 2016 *IEEE Trans. Electron Devices* **63** 4693–701
- [18] Banerjee A, Vanmeerbeek P, Schepper L D, Vandeweghe S, Coppens P and Moens P 2016 *IEEE Int. Reliability Physics Symp. (Pasadena, CA)* (<https://doi.org/10.1109/IRPS.2016.7574585>)
- [19] Qi Y, Zhu Y, Zhang J, Lin X, Cheng K, Jiang L and Yu H 2018 *IEEE Trans. Electron Devices* **65** 1759–64
- [20] Jauss S A, Hallaceli K, Mansfeld S, Schwaiger S, Daves W and Ambacher O 2017 *IEEE Trans. Electron Devices* **64** 2298–305
- [21] Higashi G S and Fleming C G 1989 *Appl. Phys. Lett.* **55** 1963–5
- [22] Spahr H, Bülow T, Nowak C, Hirschberg F, Reinker J, Hamwi S, Johannes H-H and Kowalsky W 2013 *Thin Solid Films* **534** 172–6
- [23] Bisi D *et al* 2016 *Proc. 28th Int. Symp. Power Semiconductor Devices and ICs* pp 119–22
- [24] Wang H, Wang J, Liu J, Li M, He Y, Wang M, Yu M, Wu W, Zhou Y and Dai G 2017 *Appl. Phys. Exp.* **10** 106502
- [25] Pang L, Lian Y, Kim D-S, Lee J-H and Kim K 2012 *IEEE Trans. Electron Devices* **59** 2650–5
- [26] Brown R, Macfarlane D, Khalidi A-A, Li X, Ternent G, Zhou H, Thayne I and Wasige E 2014 *IEEE Electron Device Lett.* **35** 906–8
- [27] Lee M-K, Ho C-L and Zeng J-Y 2008 *Electrochem. Solid-State Lett.* **11** D9–12
- [28] Sze S M 1967 *J. Appl. Phys.* **83** 2951–6
- [29] Wu T-L *et al* 2015 *Appl. Phys. Lett.* **107** 093507
- [30] Yang S, Liu S, Lu Y, Liu C and Chen K J 2015 *IEEE Trans. Electron Devices* **62** 1870–8
- [31] Bao Q *et al* 2016 *Semicond. Sci. Technol.* **31** 065014
- [32] Qin X, Lucero A, Azcatl A, Kim J and Wallace R M 2014 *Appl. Phys. Lett.* **105** 011602
- [33] Yang S, Tang Z, Wong K-Y, Lin Y-S, Lu Y, Huang S and Chen K J 2013 *IEDM Technical Digest* pp 6.3.1–4
- [34] Hashizume T, Ootomo S, Inagaki T and Hasegawa H 2003 *J. Vac. Sci. Technol. B* **21** 1828–38
- [35] Deen D A, Storm D F, Bass R, Meyer D J, Katzer D S, Binari S C, Lacin J W and Gougousi T 2011 *Appl. Phys. Lett.* **98** 182112
- [36] Deen D, Storm D, Meyer D, Katzer D S, Bass R, Binari S and Gougousi T 2010 *Phys. Status Solid c* **8** 2420–3
- [37] Ofuonye B, Lee J, Yan M, Sun C, Zuo J-M and Adesida I 2014 *Semicond. Sci. Technol.* **29** 095005
- [38] Saadat O I, Chung J W, Piner E L and Palacios T 2009 *IEEE Electron Device Lett.* **30** 1254–6